Journal Home Page www.bbbulletin.org

BRITISH BIOMEDICAL BULLETIN

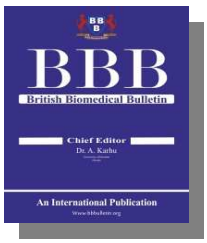

Original

Investigation on the Binding Affinities of Different Anthelmintic Drugs on the 3D Model Protein Structure of Acetylcholinesterase of *Schistosoma mansoni*: An *in silico* Approach

Ananta Swargiary*[1] and Akalesh Kumar Verma[2]

[1]*Department of Zoology, Bodoland University, Kokrajhar, Assam, India*
[2]*Department of Molecular Oncology, Cachar Cancer Hospital and Research Centre, Meherpur, Assam, India*

ARTICLE INFO

Received 03 Jan. 2015
Received in revised form 20 Jan. 2015
Accepted 23 Jan. 2015

Keywords:
Schistosoma mansoni,
Acetylcholinesterase,
3D structure,
Anthelmintic,
Docking

Corresponding author: Department of Zoology, Bodoland University, Kokrajhar, Assam, India.
E-mail address: ananbuzoo101@gmail.com

ABSTRACT

Objective: Acetylcholinesterase (AchE) is an important neurotransmitter enzyme that helps in the motility of helminth parasites. In view of functional significance, the present study was designed to predict three dimensional (3D) structure of *Schistosoma mansoni* AchE and study the binding affinity of ten anthelmintics with the model protein.
Methods: Protein models were generated using Modeller9v10, taking 2PM8 template protein. PROCHECK, ANOLEA and ERRAT tools were used to validate the model proteins. Anthelmintics-albendazole (ABZ), artemether (ART), benzimidazole (BZD), diethylcarbamazine (DEC), levamisole (LEV), mebendazole (MBZ), praziquantel (PZQ), oxamniquine (OXA), metrifonate and phosphonic amides were studied for its binding affinity against the modeled protein using Molegro Virtual Docker taking two natural AchE-inhibitors, eserine and tetra-isopropyl pyro phosphamide as a reference drug. Similarly, identification of the lead compound among all the 12 ligands has also been performed using PharmaGist.
Results: Five model proteins were generated in this present study. Out of the 5 homology protein models, model protein number 5 was chosen to be best on the basis of the result of various validation tools used. Ligand binding pockets search by CASTp showed a total 152 pockets with best pocket with an area and volume 2964.8 and 6480.3Å, respectively. Superpositions and multiple flexible alignments of a random set of 10, 5 and 3 annotated ligands by the server generated tetra-isopropyl pyro phosphamide, ABZ and MBZ as the lead compounds amongst all ligands. Superimposition of 3 annotated ligands revealed MBZ the best pharmacophore ligand with top score 22.35. Docking studies showed MBZ having the highest binding affinity followed by ABZ and PZQ. Reference drugs showed similar kind of affinity

with the model protein.
Conclusion: The present study appears to provide greater inside about the functioning of AchE of *S. mansoni* and its interaction with different anthelmintic drugs.

Introduction

Helminth parasites exhibit diversity of intercellular signaling molecules. Like other animals, acetylcholinesterase which catalyze hydrolysis of acetylcholine (Ach) neurotransmitter is one of the most important enzymes[1]. Biochemical and histochemical studies have revealed the presence of AchE in many helminth parasites including flatworms. The presence of choline and choline acetyltransferase, has also been revealed in many parasites[2]. The importance of AchE and its physiological role in nerve transmission is well known in higher organisms, however, it is unexplored in helminth parasites[3]. The motility and survival strategy of helminths are controlled by proper neuromuscular coordination system and any interference to this system could lead to the paralysis and expulsion from the host body or even death of the parasite[4]. During nerve transmission, AchE hydrolyzes Ach to choline and acetate at the synaptic cleft[5]. In trematodes, AchE is found to be associated with surface teguments and internal sub-cellular structures[6]. Because of its physiological significance, AchE has been a target of many drugs and poisons, both natural and synthetic[7].

A large number of drugs and photochemical have been investigated to see their interference on AchE activity[8,9]. However, most of the earlier motility study was done by direct observations of their motility by electronic micromotility meter[10]. Although, helminth neuromuscular system is known as analogous to their vertebrate host, very little is known about its functioning in helminth parasites which draws attention of the scientific community to develop anthelmintic drugs which is still an insufficient and difficult process[11]. Therefore, in order to know probabilities of the drug's efficacy and its mechanism of action, the present study was designed to generate the *in silico* 3D structure of AchE enzyme and to evaluate its binding affinity with different anthelmintic drugs.

Materials and Methods

Drugs

The 3D structure of all the 10 anthelmintic drugs viz., albendazole, artemether, benzimidazole, diethyl-carbamazine, mebendazole, metrifonate, oxamniquine, phosphonic amides, levamisole and praziquantel and two AchE-inhibitors eserine and tetra-isopropyl pyro phosphamide were retrieved from NCBI.

Sequence and template retrieval

The FASTA sequence of *S. mansoni* AchE (acc. no. AAQ14321) was retrieved from NCBI database[12]. Basic Local Alignment Search Tool (BLAST)[13] was used for searching sequence similarity. Multiple sequence alignment was performed by ClustalW[14].

Homology modeling

The 3D model protein structure of AchE was generated by comparative homology modeling of best template protein (2PM8_A) using Modeller9v10[15].

Model validation

Verifications of all the model structures generated by Modeler9v10 were done using several model validation tools like, PROCHECK[16], atomic non-local environment assessment (ANOLEA)[17] and joint centre for structural genomics (JCSG)[18]. The best refined model was compared with the template protein by superimposition through Chimera[19].

Pharmacophore detection study

The lead compound among the twelve ligands was generated by PharmaGist[20]. The input file (.mol2) containing all the ligands when submitted to the server, a list of candidate pharmacophores sharing the 3D-patterns of physicochemical features were generated. The best pharmacophore ligand was chosen based on alignment scores.

Active site prediction and molecular docking

The refined model protein was submitted to CASTp[21] to locate the probable active sites. Docking was performed using Molegro Virtual Docker and proper bonds, bond orders, hybridization and charges were assessed. Ten runs were performed and five poses returned. Other docking parameters were set as default.

Results and Discussion

Sequence alignment and homology modeling

The FASTA sequence of Acetylcholinesterase of *S. mansoni* retrieved from NCBI has 687 amino acid sequences. An appropriate template for query sequence was identified based on E-value, % sequence coverage and % sequence identity. The crystal structure of recombinant full length human butyrylcholinesterase (Chain-A, pdb ID - 2PM8-A, amino acid 574) was found to be the best template for the query sequence in Protein Data Bank with maximum and total score 338 each, 88% query coverage, E-value $2e^{-103}$ and maximum sequence identity 35%[22]. Other pdb hits in BLAST search were rejected based on their low % sequence identity, less query coverage and high E-value. The multiple sequence alignment using ClustalW is shown below (Fig. 1). No sequence alignments were observed between the template and modelled protein up to the 66th residue. Similarly, stretches of gap regions were seen in between the sequences of template protein and query sequences. Likewise, the AchE of diverse organisms was found to share 34% identity and 47% similarity with ACE-1 of *Caenorhabditis elegans*[23].

Model 5 has been selected as the best model based on the amino acid distribution in Ramachandran plot, mainly in the disallowed region (Table 1). Only 0.7% residues were found to be distributed in disallowed region compared to 1.0, 1.3, 1.7 and 2.6% in model 1, 2, 3 and 4, respectively. The crystal structure of template protein showed 0.6% residues in disallowed region. All the non-refined models generated by modeler9v10 were submitted to ANOLEA which gave a high score of more than >5000 in all the models. However, compared to other models, the refined model showed much better score -1642 (Table 1) but higher than template structure (ANOLEA score = -4041).

The Ramachandran plot of the refined model protein is shown in figure 2. Out of 687 amino acid residues 475 (78.6%) were distributed in the most favoured region. Similarly, 114 (18.9%) and 12 (2.0%) were found in the additional and generously allowed regions of plot, respectively. Three amino acids namely, Serine at 227 and 395 positions and Asparagine at 395 were found to be distributed in the disallowed region contributing 0.5% of the total residues. In our earlier work we tried to give the 3D

model structure of PEPCK from *Ascaris suum* and *Schistosoma mansoni* where we could bring the amino acid distribution to >90% in the core region of the plot[24].

Structural comparison and superimposition

Root mean squared deviation (RMSD) is a commonly used matrix to represent the distance between two objects which indicates the degree of similarity between two 3D structures. Lower RMSD value indicates more similarity between the structures. In our present study, superimposition of template and the refined model showed RMSD value of 0.661Å. Figure 3 compares the two protein structures and their superimposition (Fig. 4a).

A large number of deviations were observed in the loop regions and the amino acid sequences where the template has no sequence alignments with the model protein, mainly in the starting regions of the sequences (Fig. 1). The enlarged views of some of the loops were shown in figure 4b. All the four loops shown in the enlarged view were made by the model protein showing deviations from the template protein structure. Arrow 1 of the fig. 4b is a loop of 12 amino acid residues starting from 1st to 12th residue of model protein. Similarly, in a crystal structure of *Drosophila melanogaster*[25], some of the surface loops were found to be deviated by up to 8 Å from their position in the vertebrate structures. Likewise, the loops shown by arrow 2, 3 and 4 were made up of 18 (17-34), 44 (48-92) and 7 (174-180) residues, respectively. The structural deviations of *S. mansoni* AchE model protein may be related to the difference of amino acids with the sequence of template protein. A phylogenetic tree constructed from AchE sequences from *Schistosoma sp*. and other organisms revealed a distinct clade which is separate from the AchEs of other phyla. Within the clade, *S. bovis* and *S. haematobium* AchE showed more closeness other than the *S. mansoni* AchE[12].

Active site prediction and molecular docking studies

The refined 3D protein structure of *S. mansoni* AchE was submitted to the online CASTp server using its default settings of 1.4Å radius which generated 152 numbers of ligand binding pockets. Out of the 152 binding pockets, pocket number 152 and 151 were found to be the best sites with the areas of 2964.8Å and 1495.0Å and volumes of 6480.3Å and 2556.1Å, respectively. A wireframe structural display with red colored backbone and green (pocket number 152) and blue colored pocket (no. 151) were shown in the figure 5. The amino acid arrangements of the pockets were also shown in the right side of the figure.

Pharmacophore is the spatial arrangement of features that is essential for a molecule to interact with a specific target receptor[26]. Six standard pharmacophore features viz., H-bond acceptor and donor group, positive and negative ionisable group, hydrophobicity and their aromatic rings were taken into consideration for the detection of lead compound. The first selected pharmacophore candidate (Fig. 6a) developed in the present study by multiple alignment of ten drugs/inhibitors consists of 3 features - one hydrophobic and two H-bond acceptors (Fig. 6b). The second pharmacophore (Fig. 6c) candidate and its corresponding multiple alignment (Fig. 6d) showed that pharmacophore model consisted of one aromatic ring, one H-bond donor and two H-bond acceptor groups. The third pharmacophore (Fig. 6e) candidate and its corresponding multiple alignment (Fig. 6f) shows that the pharmacophore model consists of two aromatic rings, one donor, one acceptor and one positive charged group, which is the top scoring pharmacophore. It has been observed that the 3 ligands

pharmacophore consisting of MBZ, ABZ and BZD secured top score (22.35) among all the alignments (Table 2) indicating MBZ the best ligand.

Molecular docking has revealed MBZ having the highest binding affinity with the modeled protein followed by ABZ and PZQ. The MolDock and Rerank score of MBZ were -123.26 and -105.48, respectively with H-bond score of -4.59. There were 3-H-bonds having 3.48Å, 2.84Å and 2.92Å bond length (Table 3). Oxamnaquine was found to form 5 H-bond interactions with the model protein, while the Rerank score is -76.16 compared to -105.48 in the MBZ. Lowest binding affinity was observed in metrifonate with Rerank score of only -52.2 showing 3 H-bond interactions. Docking result with the known inhibitor (eserine and tetra-isopropyl pyro phosphamide) produced similar binding affinity with rerank score of about -85 and -83, respectively (Table 3). The presence of non-specific cholinesterase and specific AchE and their inhibition on exposure to drugs like iso-OMPA, serine, phenothiazine, piperazine, and p-rosaniline was detected in *A. suum*[27]. Investigation on acetylcholinesterase activity of *Ascaridia galli* and its kinetic properties revealed inhibition of AchE activity on exposure of the worm to commercial anthelmintics drugs piperazine, adipate and ABZ[28]. Wet lab studies by Alonso-Villalobos and Martinez-Grueiro[29] have shown a significant inhibition of AchE secretion in culture media when the parasite, *Heligmosomoides polygyrus* was incubated with several broad-spectrum anthelmintics like ABZ, MBZ, LEV, ricobendazole, morantel or ivermectin (IVM). The inhibition profile of three form of AchEs (BxACE-1, BxACE-2, and BxACE-3) of *Bursaphelenchus xylophilus* revealed dose-dependent inhibition of BxACE-1 by α-pinene, BxACE-3 activity was inhibited by both α-pinene and limonene whereas BxACE-2 was not inhibited by either of these inhibitors[30]. Similarly, *in-vitro* studies with the commercial anthelmintic PZQ inhibited the AchE activity up to more than 50% in fluke parasite *F. buski*[6].

The H-bond forming amino acids lying around MBZ was Ser-94, Arg-83 and Cys-80, respectively (Fig. 7a). Similarly, the amino acids around the AchE inhibitor, Eserine and Tetra-isopropyl pyro phosphamide were Cys-80, Asn-48, Ser-50, Gln-557, Phe-558 and Ile-47, Val-76 and Phe-554 respectively (Fig. 6,7b). However, it was surprising to see that all these amino acids in the active sites mentioned drugs have also been seen in the predicted active site (pocket: 152) of the model protein (Figure 5). Similar kind of work involving inhibitory activity of tacrine against the AchE revealed that the binding model of tacrine was found to sandwich between the rings of Phe-330 and Try-84 and its aromatic phenyl and pyridine rings showing parallel π-π bond interaction with the phenyl ring of Phe-330 forming average distances of 3.4 and 3.6 Å[31], respectively. Likewise, Kapkova *et al*[32] performed docking experiment to explore the binding affinity of various synthetic ligands of bispyridinium type with the homology modeled AchE enzyme and observed many interactions like π-π stacking and cation-π contacts with amino acid residues of the anionic substrate binding site (Trp-84, Phe-331, and Tyr-334) and the peripheral anionic binding site (Trp-279). Docking analysis with two alkaloids namely (+)-buxabenzamidienine and (+) - buxamidine isolated from *Buxus sempervirens* also showed good interaction with the active site of human AchE including several other hydrophobic interactions[33]. Recently, Chen *et al*[34] working on 3D model structure of human AchE build by using crystal structure of *T. californica* AchE and docked with the AchE inhibitors like Donepezil, Evo9, 10 and 27 showed a good interaction of inhibitors at the active site of the protein.

Conclusion

The present study predicts the 3D homology protein model structure of *Schistosoma mansoni* acetylcholinesterase enzyme based on the known crystal structure of full length Human Butyrylcholinesterase, their probable ligand binding sites and plausible functional and binding affinities of ten commercial anthelmintics including two AchE-inhibitors with the model protein. The model protein when superimposed with the template protein results RMSD score 0.661Å indicating less deviations between the two proteins. Large numbers of loops deviating from the template protein may be because of the less sequence similarities (only 35%) between the two proteins. Therefore, it may also be suggest that the AchE-inhibitory activity of different commercial drugs in helminth parasites may have no effect on human AchE which has far more different sequence similarity. Large differences in the sequences of amino acid may also suggest the functional differences in both the organisms. Docking studies showed good binding affinity with all the ligands forming H-bonds with almost all the nearby amino acids of the model protein as predicted by CASTp server. Based on the rerank score, it can be suggest that mebendazole showed the highest binding affinity with AchE followed by ABZ, PZQ and OXA. Docking result with the known inhibitor (eserine and tetra-isopropyl pyro phosphamide) produced similar results with rerank score of about -85 and -83 respectively. Thus, mebendazole and albendazole showing more binding affinity with AchE as compared to the known inhibitors, eserine and tetra-isopropyl pyro phosphamide justify their use as broad spectrum for human and veterinary animals.

References

1. Van Belle D, De Maria L, Iurcu G *et al.* Pathways of ligand clearance in acetylcholinesterase by multiple copy sampling. *J Mol Biol*. 2000; 298:705-726.
2. Sukhdeo MVK, Sangster NC, Mettrick DF. Effects of cholinergic drugs on longitudinal muscle contractions of *Fasciola hepatica*. *J Parasitol*. 1986; 72:858-864.
3. Lu S, Wu JW, Liu H *et al*. The discovery of potential acetylcholinesterase inhibitors: A combination of pharmacophore modeling, virtual screening, and molecular docking studies. *J Biomed Sci*. 2000; 18:1-13.
4. Mansour TE. Chemotherapeutic Targets in Parasites: Contemporary Strategies (Cambridge University Press). 2002; 156.
5. Moczon T, Swietlikowska A. Acetylcholinesterase from mature *Hymenolepis diminuta* (Cestoda). *Acta Parasitologica*. 2005; 50:343-151.
6. Roy B, Swargiary A, Giri BR. *Alpinia nigra* (Family Zingiberaceae): An anthelmintic medicinal plant of North-East India. *Advances in Life Sciences*. 2012; 2:39-51.
7. Martin RJ. Modes of action of anthelmintic drugs. *Vet J*. 1997; 154:11.
8. Singh SK, Kaushal D, Murthy PK *et al.* Partial purification and characterization of acetylcholinesterase iso-enzymes from adult bovine filarial parasite *Setaria cervi. Indian J Biochem Biophys*. 2007; 44:397-385.
9. Swargiary A, Roy B. Kinetics of Acetylcholinesterase inhibition in *Fasciolopsis buski* and *Raillietina echinobothrida* by shoot extract of *Alpinia nigra*, an indigenous medicinal plant. *Medicinal Plants*. 2011; 3:145-150.
10. Veerakumari L, Priya P. *In vitro* effect of azadirachtin on the motility and acetylcholinesterase activity of *Cotylophoron cotylophorum* (Fischoeder, 1901). *Journal of Veterinary Parasitology*. 2006; 20:1-5.
11. Geary TG, Klein RD, Vanover L *et al.* The nervous systems of helminths as targets for drugs. *J Parasitol*. 1992; 78:215-230.
12. Bentley GN, Jones AK, Agnew A. Mapping and sequencing of acetylcholinesterase genes from the platyhelminth blood fluke Schistosoma. *Gene*. 2003; 314:103-112.
13. Altschul SF, Gish W, Miller W *et al*. Basic local alignment search tool. *J Mol Biol*. 1990; 215:403-410.

14. Russell RB, Barton GJ. Multiple protein sequence alignment from tertiary structure comparison: assignment of global and residue confidence levels. *Proteins*. 1992; 14:309-323.
15. Eswar N, Eramian D, Webb B *et al.* Protein structure modeling with Modeller. *Structural Proteomics Methods Mol Biol*. 2008; 426:145-159.
16. Laskowski RA, MacArthur MW, Moss DS *et al.* PROCHECK: a program to check the stereochemical quality of protein structures. *J Appl Cryst*. 1993; 26:283-291.
17. Melo F, Feytmans E. Assessing protein structures with a non-local atomic interaction energy. *J Mol Biol*. 1998; 277:1141-1152.
18. Elsliger MA, Deacon AM, Godzik A *et al.* The JCSG high-throughput structural biology pipeline. *Acta Crystallogr Sect F Struct Biol Cryst Commum*. 2010; F66: 1137-1142.
19. Laskowski RA, Rullmann JAC, MacArthur MW *et al.* AQUA and PROCHECK-NMR: programs for checking the quality of protein structures solved by NMR. *J Biomol NMR*. 1996; 8:477-486.
20. Schneidman-Duhovny D, Dror O, Inbar Y *et al.* PharmaGist: A webserver for ligand-based pharmacophore detection. *Nucleic Acids Res*. 2008; 36:223-228.
21. Binkowski TA, Naghibzadeh S, Liang J. CASTp: computed atlas of surface topography of proteins. *Nucleic Acids Res*. 2003; 31:3352-3355.
22. Ngamelue MN, Homma K, Lockridge O *et al.* Crystallization and X-ray structure of full-length recombinant human butyrylcholine-sterase. *Acta Crystallogr Sect F Struct Biol Cryst Commun*. 2007; 63:723-727.
23. Arpagaus M, Fedon Y, Cousin X *et al*. cDNA sequence, gene structure, and in vitro expression of ace-1, the gene encoding acetylcholinesterase of class A in the nematode *Caenorhabditis elegans*. *J Biol Chem*. 1994; 269(13):9957-9965.
24. Swargiary A, Verma AK, Sarma K. Homology modeling and docking studies of phosphoenolpyruvate carboxykinase in *Schistosoma mansoni*. *Med Chem Res*. 2013; 22:2870-2878.
25. Harel M, Kryger G, Rosenberry TL *et al*. Three-dimensional structures of *Drosophila melanogaster* acetylcholinesterase and of its complexes with two potent inhibitors. *Protein Science*. 2000; 9:1063-1072.
26. Dror O, Schneidman-Duhovny D, Inbar Y *et al*. Novel approach for efficient pharmacophore-based virtual screening: method and applications. *J Chem Inf Model*. 2009; 49:2333-2343.
27. Hutchinson GW, Probert AJ. *Ascaris suum*: Kinetic properties, tissue specificity and ultrastructural location of cholinesterases. *Exp Parasitol*. 1972; 32(1):109-116.
28. Gupta S, Sanyal SN, Duggal CL. Study of the acetylcholinesterase activity of *Ascaridia galli*: kinetic properties and the effect of anthelmintics. *Acta Vet Hung*. 1991; 39(3-4):165-174.
29. Alonso-Villalobos P, Martinez-Grueiro MM. The *in-vitro* secretion of acetylcholinesterase by adult stages of *Heligmosomoides polygyrus*: the effects of broad spectrum anthelmintics. *J Vet Med B Infect Dis Vet Public Health*. 2000; 47:1-8.
30. Kang JS, Lee D-W, Koh YH, Lee SH. A soluble acetylcholinesterase provides chemical defense against xenobiotics in the pinewood nematode. *PLoS ONE*. 2011; 6(4): e19063. doi:10.1371/journal.pone.0019063.
31. Badran MM, Hakeem MA, Abuel-Maaty SM *et al.* Design, Synthesis, and molecular-modeling study of aminothienopyridine analogues of tacrine for Alzheimer's disease. *Arch Pharm*. 2010; 343:590-601.
32. Kapkova P, Stiefl N, Sürig U *et al.* Synthesis, biological activity, and docking studies of new acetylcholinesterase inhibitors of the bispyridinium type. *Arch Pharm*. 2003; 336:523-540.
33. Orhan IE, Khan MTH, Erdem SA *et al.* Selective cholinesterase inhibitors from *Buxus sempervirens* L. and their molecular docking studies. *Curr Comput Aided Drug Des*. 2011; 7:276-286.
34. Chen P, Tsai C, Ou C *et al.* Computational analysis of novel drugs designed for use as acetylcholinesterase inhibitors and histamine H3 receptor antagonists for Alzheimer's disease by docking, scoring and de novo evolution. *Mol Med Rep*. 2012; 5:1043-1048.

Table 1. Comparative values of Procheck and ANOLEA (E/kT) scores of all the five models with template protein and the best refined model

	Validation tools	Template	Model-1	Model-2	Model-3	Model-4	Model-5	Refined model
PROCHECK	Ramachandran plot	C=80.6% A=18.2% G=0.7% D=0.6%	C=80.5% A=15.1% G=3.5% D=1.0%	C=82.8% A=13.4% G=2.5% D=1.3%	C=79.8% A=15.9% G=2.6% D=1.7%	C=81.6% A=13.6% G=2.2% D=2.6%	C=82.6% A=14.2% G=2.5% D=0.7%	C=78.6% A=18.9% G=2.0% D=0.5%
	Varify3D	95.67%	65.70%	66.86%	67.73%	62.21%	59.01%	61.34%
	ERRAT	87.84	37.14	37.54	37.56	37.30	36.25	70.61
ANOLEA	E/kT	- 4041	7985	5102	6846	6547	7107	-1642

C = Core region, A = Allowed Region, G = generously allowed, D = Disallowed region.

Table 2. Table displaying the parts of the main output page obtained from an input with all the twelve drugs/inhibitors

No. of ligand molecules aligned	Names of the drug molecules align	No. of features	Features	Align score
10	Tetra-isopropylpyrophosphamide, albendazole, artemether, mebendazole, metrifonate, phosphinic amides, diethylcarbamazine, praziquantel, oxamniquine, eserine, levamisole	3	Hydrophobic and acceptor group	9.900
5	Albendazole, benzimidazole, mebendazole, oxamniquine, eserine	3	Aromatic, donor and acceptor	16.971
3	Mebendazole, albendazole, benzimidazole	5	Hydrophobic, donor, acceptor, positive and aromatic	22.352

Table 3. Table showing docking score, H-bond and interacting amino acid in the active site of AchE with all the anthelmintic drugs including two AchE-inhibitors

Ligands							H-bond	AchE (Chain A)		
	MolDock score	Rerank score	H-bond	Interactions	Atom name	Atom ID	(Å)	Atom name	Atom ID	Amino acid
Albendazole	-114.454	-89.51	-5	3	N(7)	4	2.51	H(1)	5916	Thr 45
					N(7)	4	3.04	H(1)	6242	Ala 93
					H(1)	26	3.08	O(8)	698	Gly 91
Artemether	-63.94	-47.94	-1.16	4	O(8)	0	3.44	H(1)	6165	Tyr 79
					O(8)	0	3.53	H(1)	5948	Asn 49
					O(8)	3	2.92	H(1)	6165	Tyr 79
					O(8)	4	3.22	H(1)	6146	Ile 78
Benzimidazole	-67.89	-57.96	-2.5	1	H(1)	9	2.76	O(8)	4454	Ser 555
Diethylcarbamazine	-79.11	-63.25	-1.43	1	O(8)	0	3.02	H(1)	5946	Asn 48
Mebendazole	-128.4	-105.48	-4.59	3	H(1)	0	3.48	O(8)	713	Ser 94
					H(1)	2	2.84	O(8)	620	Arg 83
					O(8)	26	2.92	H(1)	606	Cys 80
Metrifonate	-60.577	-52.20	-2.93	3	H(1)	13	2.71	O(8)	4448	Phe 554
					O(8)	6	3.17	H(1)	10000	Arg 510
					H(1)	13	3.02	O(8)	4436	Pro 553
Oxamniquine	-89.091	-76.16	-9.15	5	O(8)	0	3.11	H(1)	6254	Gly 91
					O(8)	0	3.08	H(1)	6248	Asn 90
					H(1)	40	3.23	O(8)	678	Trp 88
					H(1)	27	2.89	O(8)	368	Asn 48
					O(8)	2	2.88	H(1)	6242	Ala 93
Phosphonic Amides	-69.09	-64.34	-2.5	1	H(1)	34	2.99	O(8)	368	Asn 48
Praziquantel	-9504	-79.28	-0.76	2	O(8)	1	3.45	H(1)	1257	Arg 83
					O(8)	0	2.69	H(1)	1208	Tyr 79
Levamisole	-86.33	-71.53	-1.5	1	N(7)	1	3.29	H(1)	6166	Cys 80
Eserine	-108.19	-84.81	-2.35	6	O(8)	0	3.41	H(1)	5947	Asn 48
					O(8)	1	2.87	H(1)	5946	Asn 48
					O(8)	1	3.07	H(1)	5954	Ser 50
					O(8)	1	2.33	H(1)	5958	Ser 50
					H(1)	37	3.45	O(8)	4470	Gln 557
					H(1)	37	3.18	O(8)	4481	Phe 558
Tetra-isopropylpyrophosphamide	-118.57	-82.81	-4.77	4	H(1)	26	2.68	O(8)	363	Ile 47
					H(1)	25	2.69	O(8)	577	Val 76
					O(8)	3	3.42	H(1)	6134	Val 76
					H(1)	28	3.49	O(8)	4448	Phe 554

The unit of H-bond and docking score in Molegro Virtual Docker software is an arbitrary unit, lower the value better is the binding affinity.

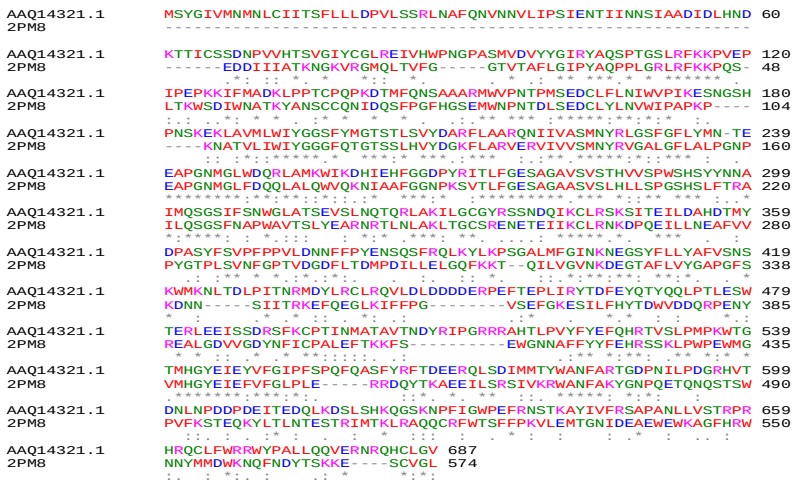

Figure 1. The pairwise sequence alignment between the FASTA sequences of 2PM8_A and *S. mansoni* AchE

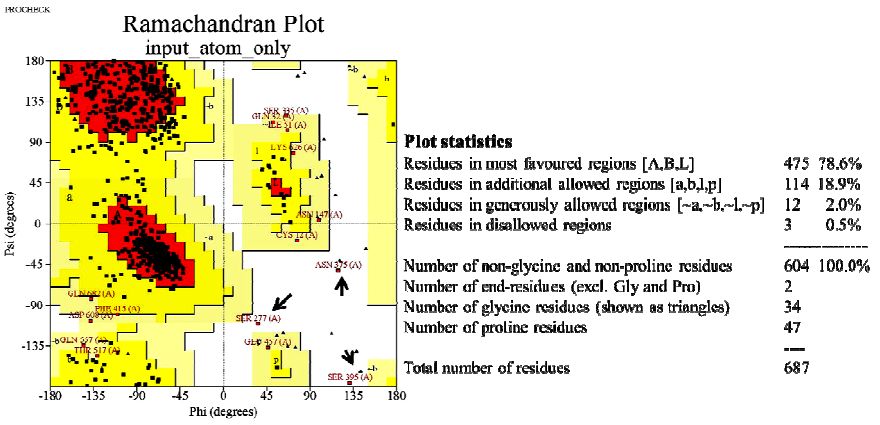

Figure 2. Ramachandran plot showing the distribution of amino acid residues and its' plot statistics. Arrows showing residues Ser-277, Asn-375 and Ser-395 in the disallowed region

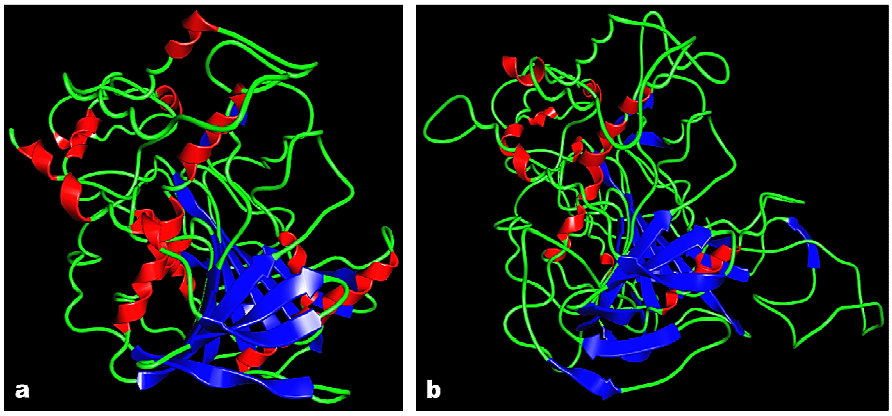

Figure 3. Tertiary protein structures - (a) Template and (b) Refined model protein of AchE of *S. mansoni*

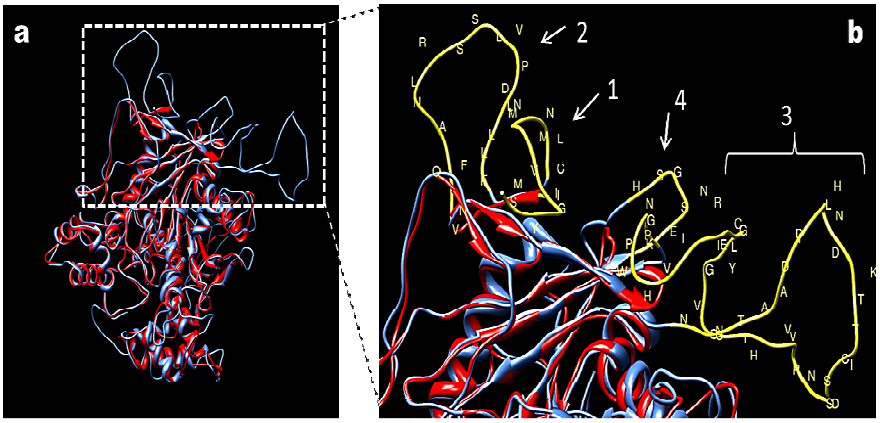

Figure 4. Superimposition of the protein structures using chimera; (a) template (red color) and model protein (cyan color), and (b) Enlarged view of superimposition showing the deviations mainly in the loop regions (yellow color)

 ISSN-2347-5447

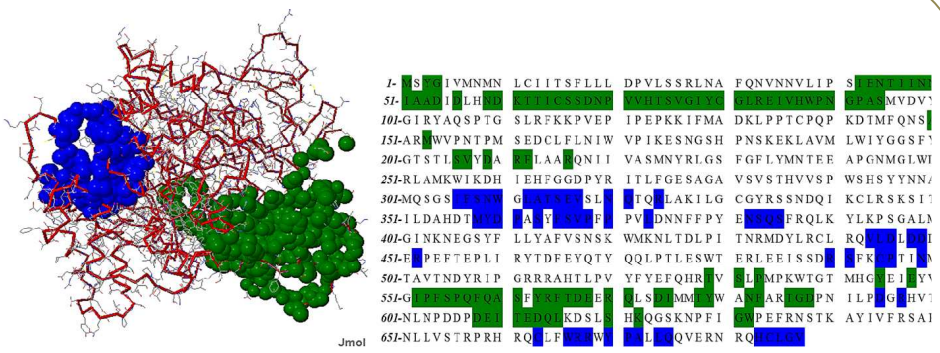

Figure 5. CASTp result showing the active sites of AchE protein model of *S. mansoni*. Only two ligand binding sites, pocket no. 152 (green) and 151 (blue) were shown with their amino acid residues at their active sites in the right side (Jmol view)

 ISSN-2347-5447

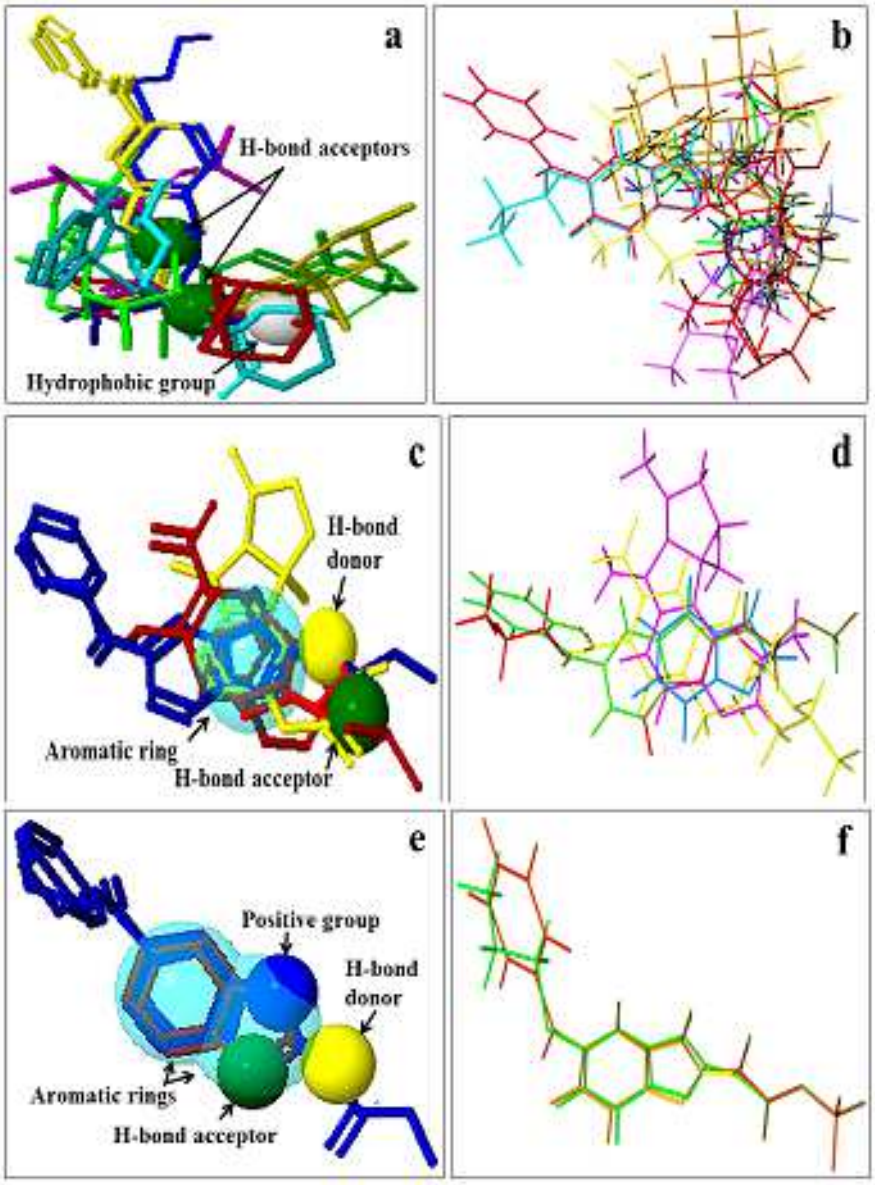

Figure 6. Pharmacophore candidates and its' corresponding multiple alignments of ligands. These were computed by PharmaGist on a random set of 10, 5 and 3 annotated ligands. (a) Showing the lowest scoring candidate pharmacophore shared by ten AchE binding drugs/inhibitors (Jmol view), (b) multiple alignments of the ten ligands in thin stick vies of (c) Showing the second highest scoring candidate pharmacophore shared by five AchE binding drugs/inhibitors. (e) Showing the top scoring candidate pharmacophore shared by three AchE binding drugs/inhibitors. Figure b, d and f showing pivot molecules after multiple alignments of 10, 5 and 3 ligands in thin-stick view of Molegro Molecular Viewer, respectively

 ISSN-2347-5447

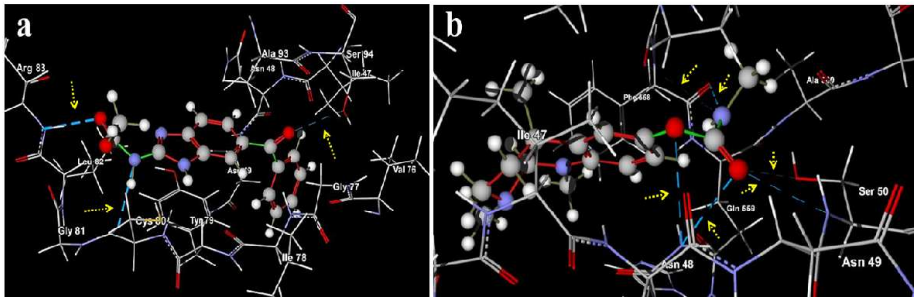

Figure 7. Docking view showing the H-bond interaction between the ligands (a. mebendazole and b. Eserine) and the model protein AchE. Dotted arrows showing the H-bonds. Proximity of amino acid residues from ligand is ≤ 4 Å